Hydrol. Earth Syst. Sci. Discuss., 6, 2099–2127, 2009
www.hydrol-earth-syst-sci-discuss.net/6/2099/2009/

Hydrology and
Earth System
Sciences
Discussions

Footprint issues in scintillometry over heterogeneous landscapes

W. J. Timmermans[1], **Z. Su**[2], **and A. Olioso**[2]

[1]International Institute for Geo-information Sciences and Earth Observation, Department of Water Resources, Box 6, 7500 AA, Enschede, The Netherlands
[2]UMR 1114 INRA-UAPV Environnement Méditerranéens et Modélisation des AgroHydrosystèmes (EMMAH), Site Agroparc, Domaine St. Paul 84914 Avignon Cedex 9, France

Received: 14 February 2009 – Accepted: 17 February 2009 – Published: 9 March 2009

Correspondence to: W. J. Timmermans (timmermans@itc.nl)

Published by Copernicus Publications on behalf of the European Geosciences Union.

Abstract

Scintillometry is widely recognized as a potential tool for obtaining spatially aggregated sensible heat fluxes. Although many investigations have been made over contrasting component surfaces, few aggregation schemes consider footprint contributions. In this paper an approach is presented to infer average sensible heat flux over a very heterogeneous landscape by using a large aperture scintillometer. The methodology is demonstrated on simulated data and tested on a time series of measurements obtained during the SPARC2004 experiment in Barrax, Spain. Results show that the two-dimensional footprint approach yields more accurate results of aggregated sensible heat flux than traditional methods.

1 Introduction

Spatial variation in surface sensible heat fluxes is a critical factor in producing and modifying regional atmospheric circulations (Avissar and Pielke, 1989) and has been a major subject of research during the past two decades (Chehbouni et al., 2000). Nowadays remote sensing algorithms are widely used for estimating these spatially distributed surface fluxes. To validate these algorithms, ground truth data are required that are directly comparable to the flux estimates obtained from such algorithms. The increasing popularity of using a large aperture scintillometer (LAS) for doing so can be explained by both its ease of operation and relatively low cost as well as by its potential capability of obtaining spatially aggregated flux estimates. However, this validation exercise is not as straightforward as one may hope for, due to mainly two issues that are related to the spatial heterogeneity of both the surface and the fluxes.

A first complication is due to the fact that although over homogeneous terrain this methodology has proven to provide accurate estimates of sensible heat (Pauwels et al., 2008; Watts et al., 2000; Meijninger and de Bruin, 2000; McAneney et al., 1995; de Bruin et al., 1995), it is also well-known that some problems of theoretical nature are faced when applying the scintillation technique over a heterogeneous surface (Ezzahar et al., 2007; Lagouarde et al., 2002a; Chehbouni et al., 2000; Bsaïbes et al., 2006).

Apart from these problems that are related to applying the scintillation technique over heterogeneous areas as such, a second problem relates to the direct comparison between the remote sensing-based and ground-based estimate of sensible heat flux. If the surface is heterogeneous, the signal measured by the sensor, the LAS in this case, depends on which part of the surface has the strongest influence on the sensor, and thus on the location and size of its so-called footprint (Schmid, 2002). In most natural landscapes, the footprint will contain different landcover types and a successful interpretation of the measured fluxes will depend on an appropriate footprint model (Soegaard et al., 2003). Therefore the only useful comparison between remote sensing-based and ground-based estimates of sensible heat flux can be done by accounting for heterogeneity within the footprint.

Shuttleworth (1988) argued that the most effective way to synthesize grid-area, weighted average values of surface characteristics is to use remote sensing techniques to diagnose areas which can be treated as a particular surface type and to compute the average value of the surface characteristics assigned to each component cover weighted by its remotely sensed area-average frequency of occurrence. It is stated that “the effective area-average value of land surface parameters is estimated as a weighted average over the component cover types in each grid through that function involving the parameter which most succinctly expresses its relationship with the associated surface flux”, which is exactly what we will attempt here.

The objective of the current contribution is to verify the suitability of the LAS for producing area-average estimates of sensible heat flux and its applicability for validating spatially distributed flux estimates. A footprint-weighted approach is proposed in Sect. 2 to aggregate surface characteristics, taking into account within footprint heterogeneity by using information obtained through remote sensing, which is then tested on simulated data in Sect. 3. In Sect. 4 we apply the suggested approach over a very heterogeneous test site in Barrax, Spain, followed by a discussion on the results in

Sect. 5. The paper is concluded with some remarks in Sect. 6.

2 Scintillation technique

In this section first a summary of the physical background of the LAS measurement is provided, described also in detail in Chehbouni et al. (2000), Lagouarde et al. (2002b) and Wang et al. (1978), valid for observations over a homogeneous surface. Then a review is provided on typical problems over heterogeneous surfaces followed by a section dealing with implications for estimating fluxes from LAS observations over a heterogeneous landscape.

2.1 The homogeneous case

Large Aperture Scintillometers (LAS) provide a measurement of the structure parameter for the refractive index C_N^2 ($\mathrm{m}^{-2/3}$) derived from the intensity fluctuations of an optical beam between a transmitter and a receiver. The variance of the natural logarithm of the irradiance I incident at the receiver is given by:

$$\sigma^2_{\ln(I)} = \overline{[\ln(I) - \overline{\ln(I)}]^2} = \int_0^1 C_N^2(u) W(u) du \tag{1}$$

where the overbar is a spatial averaging, and $W(u)$ is a non-uniform, bell-shaped and symmetrical weighing function:

$$W(u) = 16\pi^2 k \cdot P \cdot \int_0^\infty K \Phi_N(K) \sin^2 \cdot \left(\frac{K^2 P u(1-u)}{2k}\right) \cdot \left(\frac{2J_1(x)}{X}\right)^4 dK \tag{2}$$

where u (–) is the normalized path distance from the transmitter, equal to x/P, with P being the path length (m). The optical wave number, $k{=}2\pi/\lambda$ and $x{=}1/2KDu$, where D

is the receiver/transmitter aperture and K the three-dimensional spatial wave number. J_1 is a Bessel function of the first kind of order one, and Φ_N, the three-dimensional Kolmogorov spectrum of the refractive index, which describes the turbulent medium in terms of its Fourier components K, is given by:

$$\Phi_N(K) = 0.033 \cdot C_N^2 K^{-11/3} \tag{3}$$

Integration of Eq. (2) combined with Eqs. (1) and (3), yields the spatial average value of the structure parameter as obtained from a LAS, following Wang et al. (1978):

$$\left\langle C_N^2 \right\rangle = 1.12 \cdot \sigma^2_{\ln(I)} \cdot D^{7/3} \cdot P^{-3} \tag{4}$$

where the brackets on the left hand side of the equation indicate a spatial average of the measured refractive index.

Several authors (de Bruin et al., 1993; Green et al., 2001; McAneney et al., 1995) have described the theory in detail for deriving turbulent exchange from scintillation measurements over uniform surfaces, which is summarized here. In the optical domain, when humidity fluctuations in the atmosphere have a much smaller influence on the signal than temperature fluctuations, the structure parameter for temperature, C_T^2 $\left(\mathrm{K}^2\,\mathrm{m}^{-2/3}\right)$ can be derived from C_N^2 as measured by a scintillometer following Wesely (1976):

$$C_T^2 = C_N^2 \left(\frac{T_a^2}{\gamma \cdot p} \right)^2 \cdot \left(1 + \frac{0.03}{\beta} \right)^{-2} \tag{5}$$

in which T_a represents air temperature (K), γ is the refractive index for air $\left(7.9\times10^{-7}\,\mathrm{K\,Pa}^{-1}\right)$, p (Pa) indicates atmospheric pressure and β (–) is the well-known Bowen ratio, here used as a correction term for humidity related scintillations. Similarity relationships (Wyngaard et al., 1971) based on Monin-Obukhov Similarity Theory, provide the possibility to derive sensible heat flux, H $\left(\mathrm{W\,m^{-2}}\right)$, through the use of the temperature scale, T_* (K), following:

$$C_T^2 = T_*^2 (z - d_0)^{-2/3} \cdot f_T\left(\frac{z - d_0}{L}\right) \tag{6}$$

where z (m) is the effective height (Hartogensis et al., 2003) of the measurement, d_0 (m) the displacement height, f_T (–) the universal stability function, and the temperature scale is defined as:

$$T_* = \frac{-H}{\rho \cdot c_p \cdot u_*} \tag{7}$$

where ρ $\left(\mathrm{kg\,m^{-3}}\right)$ is the density of air, c_P $\left(\mathrm{J\,kg^{-1}\,K^{-1}}\right)$ the specific heat of air at constant pressure and u_* $\left(\mathrm{m\,s^{-1}}\right)$ the well-known friction velocity. The form of the stability functions adopted here are taken from Green et al. (2001):

$$f_T\left(\frac{z - d_0}{L}\right) = c_{T1} \cdot \left(1 + c_{T2} \cdot \left|\frac{z - d_0}{L}\right|\right)^{-2/3} \quad \text{for } (z - d_0)/L < 0 \text{ (unstable)} \tag{8a}$$

$$f_T\left(\frac{z - d_0}{L}\right) = c_{T1} \cdot \left(1 + c_{T3} \cdot \left(\frac{z - d_0}{L}\right)^{2/3}\right) \quad \text{for } (z - d_0)/L > 0 \text{ (stable)} \tag{8b}$$

where L (m) is the Monin-Obhukov length, defined as:

$$L = \frac{u_*^2 \cdot T_a}{g \cdot k \cdot T_*} \tag{9}$$

in which g $\left(\mathrm{m\,s^{-2}}\right)$ is the gravitational constant and k (–) the von Karman constant. The constants c_{T1}, c_{T2} and c_{T3} (–) are take equal to 4.9, 6.1 and 2.4, respectively (Wyngaard et al., 1971). There is no general consensus on the stability function for stable conditions (Eq. 8b), however, in this work we use the coefficients proposed by Wyngaard et al. (1971).

Obtaining the sensible heat flux from a scintillometer measurement over homogeneous terrain thus invokes solving H from Eqs. (5)–(9). This requires the measurement of a number of additional parameters; air temperature, air pressure, Bowen ratio, displacement height and friction velocity. Since measurements of friction velocity are not generally available, independent windspeed measurements, u, at reference height z_u may be combined with an estimate of surface roughness length, z_0, following:

$$u_* = k \cdot u \cdot \left[\ln\left(\frac{z_u - d}{z_0}\right) - \psi_M\left(\frac{z_u - d}{L}\right)\right]^{-1} \tag{10}$$

where ψ_M (–) is the integrated stability function (Panofsky and Dutton, 1984), to obtain estimates of friction velocity.

Generally an estimation of the aerodynamic properties of the terrain, surface roughness length and displacement height, estimated as a fraction of canopy height, following Brutsaert (1982), ensures an accurate estimate of sensible heat flux over homogeneous terrain. However, when applied over a heterogeneous surface, comprising of two or more patches or agricultural fields, additional assumptions need to be made, which are described in more detail in the following section.

2.2 Application to a heterogeneous surface

Besides doubts on the validity of the assumption of Monin-Obhukov similarity theory below the blending height over a heterogeneous surface, problems exist as on how to parameterize an equivalent or averaged temperature scale, and friction velocity (Lagouarde et al., 2002b; Ezzahar et al., 2007), as well as how to deal with the non-linear sensitivity of the scintillometer to C_N^2 along its beam. Lagouarde et al. (2002a) presented an approach for a two-surface composite case where aggregated estimates for displacement height were obtained using:

$$\langle d \rangle = r \cdot d_1 + (1 - r) \cdot d_2 \tag{11}$$

where the brackets indicate a spatial average and r indicates the proportion of surface 1 under the beam of the scintillometer, whereas subscripts 1 and 2 refer to the two surface components, or patches, under the beam of the scintillometer. An estimate for the areal averaged roughness length is obtained from one of the two following schemes:

$$\ln\langle z_0\rangle = r\cdot\ln(z_{01}) + (1-r)\cdot\ln(z_{02}) \tag{12a}$$

$$\left(\ln\left(\frac{z-\langle d\rangle}{\langle z_0\rangle}\right)\right)^{-2} = r\cdot\left(\ln\left(\frac{z-d_1}{z_{01}}\right)\right)^{-2} + (1-r)\cdot\left(\ln\left(\frac{z-d_2}{z_{02}}\right)\right)^{-2} \tag{12b}$$

A mean windspeed then is obtained according to an aggregation scheme based on a linear transit time for an air parcel along the pathlength, resulting in:

$$\langle u\rangle = \frac{u_1\cdot u_2}{r\cdot u_2 + (1-r)\cdot u_1} \tag{13}$$

using windspeed measured over each component. Integration of the weighing function of the scintillometer from 0 to r and from $(1-r)$ to 1 provided weighting factors, W_i, with i the component number, to obtain an average value of C_N^2 assumed to originate from the two components following:

$$\left\langle C_N^2\right\rangle = W_1\cdot\left(C_N^2\right)_1 + W_2\cdot\left(C_N^2\right)_2 \tag{14}$$

Comparison versus reference values for sensible heat, obtained from sonic measurements at the two surface components weighted following the same approach as in Eq. (11), yielded small but systematic overestimation of the scintillometer-based estimates (Lagouarde et al., 2002a). A sensitivity analysis on a simple model simulating the integration methodology showed that the composition of the pathlength, the contrast in fluxes and, to a lesser extent, the aerodynamic properties of the two surface components induced deviations between scintillometer-based estimates and reference values of sensible heat flux, where an underestimation (overestimation) by the LAS depended on whether the largest field in the pathlength is the wettest (driest) part.

A similar, but slightly different, approach is described by Ezzahar et al. (2007), who estimated C_N^2 at grid scale, consisting of an olive orchard with two contrasting fields, from component LAS measurements, demonstrating that Monin-Obhukov similarity theory applies below the blending height. They obtained a grid-scale sensible heat flux, $\langle H \rangle$, following:

$$\langle H \rangle = r \cdot H_{\mathrm{LAS}-1} + (1-r) \cdot H_{\mathrm{LAS}-2} \tag{15}$$

where subscripts 1 and 2 indicate variables associated with the two surface components, or patches, and r indicates the proportion of surface 1 to the total orchard, or the total grid. Simplifying Eq. (15) to:

$$\langle u_* T_* \rangle = r \cdot u_{*1} T_{*1} + (1-r) \cdot u_{*2} T_{*2} \tag{16}$$

and combining Eqs. (5) and (8b) with Eq. (15) an expression for C_N^2 aggregated at grid was obtained:

$$\left\langle C_N^2 \right\rangle = \langle y \rangle^{-1} \cdot \left(y_1 C_{N1}^2 + y_2 C_{N2}^2 \right) \tag{17}$$

with:

$$y_i = (r_i) \frac{u_{*i} \left(1 + \frac{0.03}{\beta i}\right)^{-2} \cdot (z_{0i} - d_i)^{2/3}}{T_{*i} \cdot \left(1 + c_{T2} \frac{(z_{0i} - d_i)}{L}\right)^{-2/3}} \tag{18}$$

where i is either component 1, 2 or indicating the grid-scale average (angular brackets), and r_i=1 for $\langle y \rangle$, r_i=r for y_1 and r_i=(1−r) for y_2.

Grid-scale averages of displacement height and roughness length are then obtained in a similar way as proposed by Lagouarde et al. (2002a) through Eq. (11) and Eq. (12b), respectively.

2.3 Footprint implications

So far, we were treating the heterogeneous surface as a one-dimensional two-component area. However, when measurements are made below the blending height a portion of the upstream surface, the source area, influences the sensor. Numerous so-called footprint models are described in the literature that relate the measured flux at a certain height to the weighted spatial distribution of the surface fluxes that contribute to the measurement. Meijninger et al. (2002) described that for applying this concept to the LAS one has to combine the footprint function with the spatial weighting function of the LAS in order to estimate the relative contribution of the surface fluxes to the measured flux.

We used a simple two-dimensional footprint model that calculates the two-dimensional source strength, $F_{x',y'}$, following:

$$F_{x',y'} = \frac{F_{x'}}{\sqrt{2\pi\sigma_{y'}}} \cdot e^{-\left(y'^2/2\sigma_{y'}^2\right)} \tag{19}$$

where $\sigma_{y'}$ is the cross wind spread in the direction y' perpendicular to the wind direction (x') and $F_{x'}$ is the relative contribution per running m along the wind direction, as:

$$F_{x'} = \frac{u}{u_*} \cdot \frac{z_m}{kx'^2} \cdot e^{-(u/u_*)\cdot(z_m/kx')} \tag{20}$$

where k is von Karman constant and z_m the measuring height. The footprint model, described in detail in Soegaard et al. (2003) is then combined with the weighting function of the LAS to obtain the relative contribution of each of the contributing component surface covers, rfp_i, where the subscript i refers to a particular surface component. Spatially distributed information on surface aerodynamic properties was input to this model to account for within footprint heterogeneity. This was accomplished by using a landcover classification obtained from an ASTER image (Van der Kwast et al., 2009) in its original resolution (15 m) in combination with a look-up table. This relative footprint-weighted contribution is then used to obtain aggregated displacement height, surface roughness and structure parameter following Eqs. (11), (12a), (17) and (18), where r_i should be replaced by rfp_i.

The approach is tested in a one-dimensional manner, which implies that in this case only the LAS weighting function is influencing the footprint, on simulated data in Sect. 3. The LAS derived sensible heat flux, H_{sim}, is obtained from simulated component sensible heat fluxes, H_1 and H_2. The procedure is such that the component structure parameters, $C^2_{N,i}$, where i is either 1 or 2, are calculated from inverting the procedure outlined by Eqs. (5)–(9). These are then weighted according to Eqs. (17) and (18), using $r_{fp,i}$ in stead of r_i to simulate a $\langle C^2_N \rangle$ a LAS would have provided, which is then used to obtain the resulting H_{sim}. Following, H_{sim} is compared versus a reference sensible heat flux, H_{ref}. This reference sensible heat flux is obtained from H_1 and H_2 as:

$$H_{\mathrm{ref}} = rfp_1 \cdot H_1 + rfp_2 \cdot H_2 \tag{21}$$

where subscripts 1 and 2 refer to the different component surfaces. In Sect. 4 the aggregation approach is applied in a two dimensional manner on data (Su et al., 2008) collected during the SPARC2004 field campaign in Barrax, Spain.

3 Simulation

We simulated the case of a composite surface comprising of two plots, applying the footprint approach described above. For the sake of comparison we also show simulation results (5000 runs) for the approaches described in detail in Lagouarde et al (2002a) and Ezzahar et al. (2007).

To build on the results obtained from simulations presented in Lagouarde et al. (2002a) we chose two components with contrasting sensible heat flux and assumed similar parameter values. This meant that for plot 1 we randomly generated sensible heat fluxes between 0 and 50 W m^{-2} and for plot 2 between 350 and 400 W m^{-2}. Roughness length and displacement height were taken as 1/8 and 2/3 times the canopy height, following Brutsaert (1982), where the canopy heights for the plots were given random heights uniformly distributed between 0.015 and 1.5 m. Windspeed, u_{ref}, at reference height, z_{ref} equal to 50 m, was given random values between 0.5 and 6.0 ms^{-1}, and the contributing areas, $r_{1,2}$, were given random numbers between 0 and 1, such that their sum equalled unity. Other parameters were kept constant, available energy (necessary to calculate a Bowen ratio) equal to 450 Wm^{-2} and air temperature, T_a, equal to 301 K.

Results are presented in Fig. 1, where in the left panels the simulated fluxes are plotted versus the reference fluxes, and the right panels show the error, $H_{\mathrm{sim}}-H_{\mathrm{ref}}$, versus the contributing area, r, or rfp. A low value for r means a low contribution from plot 1. The chosen contrast in sensible heat flux resulted in differences H_1-H_2 ranging from −400 to −300 Wm^{-2}, resembling a simulation also performed by Lagouarde et al. (2002a). However, they presented their results composing H_{ref} from its components by not taking into account the weighting function of the LAS. We have plotted the results using this assumption in Fig. 1a and e, which resemble the "diamond" class in Fig. 10 of Lagouarde et al. (2002a). In addition a simulation was run where H_{ref} was composed by taking the weighting function of the LAS into account, of which the results are shown in Fig. 1b and f. Simulation results following Ezzahar et al. (2007) are given in Fig. 1c and g, whereas values obtained from the approach described in this contribution are given in Fig. 1d and h.

It is believed that an important difference between the existing approaches is that the first one, Lagouarde et al. (2002a), attempts to unravel an LAS signal, $\langle C_N^2 \rangle$, originating from two neighboring and contrasting areas, where this aggregated signal represents an LAS measurement of $\langle H \rangle$ over the two areas. Whereas the second approach, Ezzahar et al. (2007), constructs an aggregated LAS signal, $\langle C_N^2 \rangle$, originating from two neighboring and contrasting areas, where $\langle C_N^2 \rangle$ will yield an $\langle H \rangle$ that represents a spatially weighted average, or grid-scale average, sensible heat flux.

When $H_1<H_2$ and $r<(1-r)$, the approach originally suggested by Lagouarde et al. (2002a) will yield an over-estimation of H_{sim} with respect to H_{ref}, because the method does take the LAS weighting function, $W(u)$, into consideration for obtaining an aggregated C_N^2, whereas for the calculation of the reference sensible heat flux, H_{ref}, a linear weighing based on the contributing area is assumed. This systematic effect is removed when taking the weighting function into account, but still deviations are noted which can be attributed to the assumption of Eq. (14).

This problem was solved analytically by Ezzahar et al. (2007) resulting in Eqs. (17) and (18). However, when applying their approach on a LAS signal measured over a two-component contrasting surface, the reference sensible heat flux, H_{ref}, should also be estimated from the component sensible heat fluxes weighted by the weighing function of the LAS. In the case of $H_1 < H_2$ and $r < (1-r)$, the H_{ref} will be higher than the H_{sim} since the method does not incorporate the weighing function of the LAS, resulting in an underestimation of H_{sim}. This phenomenon is illustrated in Fig. 1c. and g.

When finally taking the weighting function into account for aggregating the aerodynamic properties the errors reduce to zero, see Fig. 1d. and h, meaning that the nature of the scintillometer measurements is properly simulated. It should be noted though that when applying the methodology of Ezzahar et al. (2007) and assuming H_{ref} to originate from a simple linear weighting of the component fluxes the results are similar to those presented here. However, when utilizing LAS observations for validating spatially distributed flux estimates, footprint calculations are indispensible, implying the weighting function should be taken into account.

4 SPARC2004 Experiment

Observations of water and heat fluxes (Su et al., 2008) were made during the ESA SPARC (SPectra bARrax Campaign) 2004 field experiment conducted at the Las Tiesas Experimental Farm test site at Barrax in the La-Mancha region in Spain, maintained by the Provincial Technical Agronomical Institute (ITAP).

This agricultural area, which is partly irrigated, comprises of land covers ranging from completely bare soil to fully vegetated parcels with canopy heights from several centimeter up to two meter. The area is rather flat and is situated at an average 700 m above mean sea level. The campaign took place during two weeks in mid-summer when natural surfaces are under water-stress since rainfall is mainly absent during this period. Daily minimum and maximum temperatures measured over the vineyard during the period were 14.3 and 31.6°C. Prevailing wind directions are ranging from typically south-eastern direction during morning hours, changing towards a northern direction during late afternoon. This meant that around noon, which coincided with nominal airborne and spaceborne image acquisitions, eastern winds were prevailing.

4.1 Experimental setup

The receiver of the LAS was installed at a height of 5.06 m at the north-western side of a triangular shaped vineyard ("V1" in Fig. 2) with sides measuring about 200 m each, and quite variable canopy heights, depending on age of the crops, ranging from 1.0 up to 2.0 m. The transmitter was positioned at a distance of 784 m in a harvested wheat field containing at parts dry wheat stubbles of about 0.15 to 0.20 m height. Installation height here was 4.64 m, yielding an effective measurement height of 4.85 m of the LAS, since the area is extremely flat. The agricultural field directly surrounding the LAS setup consisted of pivot-irrigated, dense cropped corn fields, bare soil (though alternated by dried hordeum), garlic and grassland, whereas at slightly larger distances a potato field and a forest nursery as well as some other cornfields and a small orchard in the northern part of the area were located. Although most of the bare soil and stubble were very dry, most crops in the area were irrigated. Particularly the relatively large corn fields were heavily irrigated, which at times resulted in stable conditions during daytime.

Due to the prevailing wind directions we assumed the main fields influencing the LAS would be "V1", "C2" and "WS", see Fig. 2. Therefore a sonic anemometer was installed at a height of 4.4 m at the western side of field "C2", measuring the fluxes from the corn during prevailing wind directions and at times from the vineyard, during western winds. Due to the rotating pivot irrigation system the sensor had to be mounted at the edge of the corn field, with average crop heights about 1.8 to 2.2 m. Another sonic anemometer was installed in the near vicinity of the LAS receiver, about 50 m from the northern edge of the vineyard, with local crop heights about 1.1 m. A third sonic anemometer measured fluxes over the dry wheat stubble, at a height of about 1.1 m, some 150 m south-east of the LAS transmitter. As such the landcover components potentially influencing the LAS observations were monitored during 6 days, from DOY 197 to 202. The observations were made just outside the fenced area of the Las Tiesas experimental farm, which gave reason to remove part of the instrumentation during night-time hours. Due to malfunctioning of some of the sonic anemometers also no continuous dataset could be obtained. However, after averaging to 10 min intervals a data set of 69 observations was produced, containing LAS as well as all three sonic measurements. This dataset was then used for the current contribution.

4.2 Input data

Parameters needed for estimating $\langle C_n^2 \rangle$ comprise of spatially aggregated available energy, net radiation minus soil heat flux, $\langle R_n - G \rangle$, air temperature $\langle T_{\text{air}} \rangle$ and friction velocity $\langle u_* \rangle$.

Here the available energy, is used for calculating the Bowen ration, needed as a correction term in Eq. (5). Since the net radiation and soil heat flux only appear in this corrective factor in an in-direct way, their accuracy is not critical (Lagouarde et al., 2002a), and as such we have used a spatially representative constant average of 450 Wm^{-2}.

For $\langle T_{\text{air}} \rangle$ we have used a measurement obtained at about 5 m over the vineyard, which is in the center of the area. In addition, simulations have indicated that spatial variation in air temperature over the area typically are in the order of 1.5 K (Timmermans et al., 2008), which we feel justifies using a single measurement. Moreover, the observation is time-averaged implying that local variations may have been reduced.

Although the development of internal boundary layers above each surface component may slightly alter the blending height concept (Wieringa, 1986), it is used here to transfer wind speed measurements taken at 4.88 (m) over the vineyard to the blending height, which is then taken as a representative aggregate windspeed, $\langle u \rangle$, for the area. Aggregated displacement height and surface roughness length were obtained from Eqs. (11) and (12a), where r is replaced by rfp. In addition, Eqs. (11) and (12a) were expanded to three components, representing the vineyard, the wheat stubble and the corn field. For the wheat the surface roughness length was estimated as the canopy height divided by 8 (Brutsaert, 1982), yielding a value of 0.03 (m).

Since the corn crops were very dense, their surface was considerably smoother than could be expected based solely on the height of the canopy (Shaw and Pereira, 1982). Analyzing measurements from the sonic anemometer over the corn during near neutral atmospheric stability conditions yielded roughness length values between 0.03 and 0.09 m, with an average of 0.068 m. The same procedure was followed for the vineyard. Here the roughness estimates were clustered around two values, depending on wind direction. Parallel to the row-orientation of the crops we found roughness values around 0.14 m, whereas perpendicular to the rows values around 0.18 m were found. Depending on wind direction either one of them was assessed to the vineyard.

Displacement height for the three landcover components was obtained by taking it equal to two-third of the canopy height for the corn and vineyard. For the harvested wheat, a displacement height equal to zero was taken, since it consisted of rather irregularly spaced wheat stubble, rendering the displacement height principle not applicable.

4.3 Results

We have applied the footprint approach using the method presented by Soegaard et al. (2003) combined with the weighting function of the LAS, $W(u)$, following Meijninger et al. (2002). Sensible heat fluxes, H_{las}, were calculated from the scintillation measurements using the aggregated parameters as described in the previous section. Values of the average sensible heat flux obtained with the scintillometer are plotted versus the reference measurements from the sonic anemometers obtained from Eq. (21) in Fig. 3.

To demonstrate the impact of the two-dimensional footprint in the current case, additional calculations were performed, assuming either a homogeneous land cover consisting of a vineyard or a wheat field, so-called zero-dimensional approaches, as well as a one-dimensional analysis, assuming a two-component surface consisting of vineyard and wheat stubble. Reference values of sensible heat flux in the homogeneous, or zero-dimensional, cases were taken from the sonic measurements taken in the respective fields, whereas in the 1-D and 2-D cases they were calculated following Eq. (21). Naturally, adding the corn component, only possible when treating the LAS measurement in a two-dimensional way, both H_{ref} and H_{las} decreased as a result of low sensible heat flux for the corn. The upper panels in Fig. 3 shows the results when assuming the LAS is measuring over a homogeneous surface, entirely consisting of vineyard (left panel) or wheat stubble (right panel). The lower panels show the results for the one-dimensional (left panel) and two-dimensional (right panel) cases. A summary of the results is provided in Table 1.

It goes without saying that ignoring the influence of the corn field in the aggregation process, obvious for the zero- and one-dimensional cases, for the current case is not realistic. Large discrepancies between H_{las} and H_{ref} are noticed in these cases and correlation coefficients were never exceeding 0.28. Dramatic improvement in both correlation coefficient and RMSD is seen when applying the two-dimensional approach, although still relatively high deviations are noticed.

An attempt is made to further improve these estimates using prior knowledge on flux contrasts between the surface components. This is discussed in the following section.

5 Discussion

When aggregating the aerodynamic properties of the surface components reasonable estimates can be obtained from the canopy heights, yielding the possibility to estimate component friction velocities assuming a sufficiently high wind speed measurement is available. If furthermore estimates of the contrast between the fluxes of the different components are available this potentially would improve the estimating of the aggregated flux, since these are then the only remaining parameters determining the relative contributions of C_{Ni}^2 in Eqs. (17) and (18) to $\langle C_N^2 \rangle$.

We have run aggregations using several different ratios of sensible heat flux which could reasonably be expected for the three land cover components. However, no reasonable results were obtained which is attributed to the high variation of the ratio between the sensible heat fluxes measured over the different fields with time. The fluxes over the vineyard and wheat stubble were rather stable for the days of observation, but rather large fluctuations for the corn were noted, most probably due to irrigation. However, to test whether improvements could be established, we have used the sonic observations of the sensible heat fluxes to determine the ratios between the fluxes and implemented these in the aggregation scheme. The results for this simulation are displayed in Fig. 4a.

Surprisingly, the results deteriorated with respect to the aggregation not using prior knowledge on flux ratios.

One of the obvious reasons is the simultaneous occurrence of unstable and stable conditions within the footprint of the LAS. Under certain conditions the irrigated cornfields created an oasis effect in the elsewhere dry and hot surroundings, causing at times stable conditions over the corn. In such cases, which are represented by a low or even negative reference flux, Eqs. (17) and (18) do not hold since the LAS cannot discriminate between upward or downward fluxes. In Fig. 4a these cases are marked by circles.

Despite careful analysis of the local circumstances and prevailing wind directions when setting up the experiment it could not be avoided that at certain moments during the campaign the footprint of the LAS included land covers no reference observations of sensible heat flux were made. Since the aggregation procedure for the aerodynamic properties demands that the sum of the relative contributions of the components is equal to unity, the values for rfp_i were normalized by dividing them by the sum of the three components actual reference measurements took place. However, during 73% (83%) of the time the three components contributed for more than 75% (50%) to the total footprint of the LAS, which we believe is acceptable. Under these circumstances one could think in the line of Hoedjes et al. (2007) and use thermal remote sensing information to produce estimates of fluxes for components that were not covered by sonic anemometers. However, this information was not available for the duration of the experiment.

Another reason for a mismatch between H_{las} and H_{ref} is attributed to incorrect component fluxes. Obviously the sonic measurements are also characterized by their respective footprints, which like the LAS footprint, is variable in time, depending mainly on wind direction. Figure 4b shows the contribution of the land cover component where the sonic anemometers were located relative to the total contributing source area as a function of wind direction. The vineyard is represented by open circles, the wheat stubble by crosses and the corn is represented by closed diamonds. It is clearly noticed that when wind directions are between 100 and 180°, resembling eastern to southern directions, the sonic footprints were most “pure”, or homogeneous.

A plot of the results of the aggregation scheme for estimating H only for wind directions between 100 and 180° are presented in Fig. 5a. Although for some points a near perfect fit is obtained, there are still a few observations that generate large discrepancies between H_{las} and H_{ref}. Since in the simulations no discrepancies between H_{las} and H_{ref} occurred, the reason here, apart from contrasting stability, must lie in the component fluxes being incorrect, or not pure, or incomplete, meaning the footprint of the LAS contained more covers than only vineyard, wheat stubble or corn.

The discrepancies between H_{las} and H_{ref} seem related to the contrast between the component fluxes, as shown in Fig. 5b. For illustration purposes the maximum ratio is set to 5 in the figure. Because of this, one outlier is not shown, which showed H component-ratios around 200 and a difference between H_{las} and H_{ref} equal to 88.5 $\mathrm{W m^{-2}}$. It appears that generally a larger contrast between the component fluxes invokes larger discrepancy between H_{las} and H_{ref}. There seems to be one exception to this, which is the point with the highest error. However, inspection learnt that this point had about 20% of its footprint not covered by any of the three surface components measured by a sonic. Moreover, the sonic of the vineyard for this particular observation only had a 48% contribution from the vineyard itself, despite a favourable wind direction.

A somewhat arbitrary threshold value seems to be present at a contrast ratio about 2. Below this value differences between H_{las} and H_{ref} are within 20 Wm^{-2}, above this value discrepancies rapidly increase. This indicates that when the surface fluxes for the different landcover components were too contrasting, the LAS measurement experienced problems.

6 Conclusions

A methodology is proposed to produce LAS-derived area-averages of sensible heat fluxes suitable for validating spatially distributed models that estimate surface fluxes. The soundness of the method is demonstrated by reproducing simulated component fluxes by model inversion. Although model results were considerably better than using traditional approaches when applied over the very heterogeneous Barrax test site, some complications are noticed.

These were partly due to the nature of the available data. During a limited number of observations both stable and unstable conditions occurred within the footprint of the LAS. Due to the nature of the measurement technique the LAS is not able to distinguish between these conditions, consequently the method does not work and the LAS estimates deviated from the reference values under these circumstances. Though limited in number, during some moments wind directions were such that the footprint of the LAS encompassed land cover units where no reference observations of sensible heat flux were available. The same phenomenon brought about that at times the footprint of the reference observations was not homogeneous. Obviously this can hardly be avoided when dealing with agricultural patches under natural conditions. However, when the contrast between land cover components is not too contrasting, deviations between LAS based estimates and reference values were within 20 Wm^{-2}.

Acknowledgements. This work has been partly funded though ESA 18307/04/NL/FF. We would like to thank A. Gieske from ITC and L. Jia and J. Elbers from ALTERRA for their help in the installation and maintenance of the ground stations.

References

Avissar, R. and Pielke, R. A.: A parameterization of heterogeneous land surfaces for atmspheric numerical models and its impact on regional meteorology, Mon. Weather Rev., 117, 2113–2136, 1989.

Brutsaert, W.: Evaporation into the atmosphere, Reidel, Dordrecht, The Netherlands, 299 pp., 1982.

Bsaïbes, A., Prévot, L., Voltz, M., Lagouarde, J.-P., and Irvine, M.: Modelling evapotranspiration at the watershed scale using a multi-local approach, European Meteorological Society, 6th EMS/6th ECAC, Ljubljana, Slovenia, 4–8 September, 2006.

Chehbouni, A., Watts, C., Lagouarde, J.-P., Kerr, Y. H., Rodriguez, J.-C., Bonnefond, J.-M., Santiago, F., Dedieu, G., Goodrich, D. C., and Unkrich, C.: Estimation of heat and momentum fluxes over complex terrain using a large aperture scintillometer, Agr. Forest Meteorol., 105, 215–226, 2000.

de Bruin, H. A. R., Kohsiek, W., and Hurk, B. J. J. M. v. d.: A verification of some methods to determine the fluxes of momentum, sensible heat, and water vapour using standard deviation and structure parameter of scalar meteorological quantities, Bound.-Lay. Meteorol., 63, 231–257, 1993.

de Bruin, H. A. R., Hurk, B. J. J. M. v. d., and Kohsiek, W.: The scintillation method tested over a dry vineyard area, Bound.-Lay. Meteorol., 76, 25–40, 1995.

Ezzahar, J., Chehbouni, A., Hoedjes, J. C. B., and Chehbouni, A.: On the application of scintillometry over heterogeneous grids, J. Hydrol., 334, 493–501, 2007.

Green, A. E., Astill, M. S., McAneney, K. J., and Nieveen, J. P.: Path-averaged surface fluxes determined from infrared and microwave scintillometers, Agr. Forest Meteorol., 109, 233–247, 2001.

Hartogensis, O. K., Watts, C. J., Rodriguez, J.-C., and de Bruin, H. A. R.: Derivation of an effective height for scintillometers: La Poza Experiment in Nortwest Mexico, J. Hydrometeorol., 4, 915–928, 2003.

Hoedjes, J. C. B., Chehbouni, A., Ezzahar, J., Escadafal, R., and de Bruin, H. A. R.: Comparison of large aperture scintillometer and eddy covariance measurements: Can thermal infrared data be used to capture footprint-induced differences?, J. Hydrometeorol., 8, 144–159, 2007.

Lagouarde, J.-P., Bonnefond, J.-M., Kerr, Y. H., McAneney, K. J., and Irvine, M.: Integrated sensible heat flux measurements of a two-surface composite landscape using scintillometry, Bound.-Lay. Meteorol., 105, 5–35, 2002a.

Lagouarde, J.-P., Jacob, F., Gu, X. F., Olioso, A., Bonnefond, J.-M., Kerr, Y., Mcaneney, K. J., and Irvine, M.: Spazialization of sensible heat flux over a heterogeneous landscape, Agronomie, 22, 627–633, 2002b.

McAneney, K. J., Green, A. E., and Astill, M. S.: Large-Aperture Scintillometry: the homogeneous case, Agr. Forest Meteorol., 76, 149–162, 1995.

Meijninger, W. M. L., Hartogensis, O., Kohsiek, W., Hoedjes, J. C. B., Zuurbier, R. M., and de Bruin, H. A. R.: Determination of area-averaged sensible heat fluxes with a large aperture scintillometer over a heterogeneous surface – Flevoland field experiment, Bound.-Lay. Meteorol., 105, 37–62, 2002.

Meijninger, W. M. L. and de Bruin, H. A. R.: The sensible heat fluxes over irrigated areas in western Turkey determined with a large aperture scintillometer, J. Hydrol., 229, 42–49, 2000.

Panofsky, H. A. and Dutton, J. A.: Atmospheric Turbulence: Models and Methods for Engineering Applications, John Wiley and Sons, New York, 397 pp., 1984.

Pauwels, V. R. N., Timmermans, W. J., and Loew, A.: Comparison of the estimated water and energy budgets of a large winter wheat field during AgriSAR 2006 by multiple sensors and models, J. Hydrol., 349, 425–440, doi:10.1016/j.jhydrol.2007.11.016, 2008.

Schmid, H. P.: Footprint modeling for vegetation atmosphere exchange studies: a review and perspective, Agr. Forest Meteorol., 113, 159–183, 2002.

Shaw, R. H. and Pereira, A. R.: Aerodynamic roughness of a plant canopy: A numerical experiment, Agr. Meteorol., 26, 51–65, 1982.

Shuttleworth, W. J.: Macrohydrology – The new challenge for process hydrology, Journal of Hydrology, 100, 31-56, 1988.

Soegaard, H., Jensen, N. O., Boegh, E., Hasager, C. B., Schelde, K., and Thomsen, A.: Carbon dioxide exchange over agricultural landscape using eddy correlation and footprint modelling, Agr. Forest Meteorol., 114, 153–173, 2003.

Su, Z., Timmermans, W. J., Gieske, A. S. M., Jia, L., Elbers, J. A., Olioso, A., Timmermans, J., Van der Velde, R., Jin, X., Van der Kwast, H., Sabol, D., Sobrino, J. A., Moreno, J., and Bianchi, R.: Quantification of land-atmosphere exchanges of water, energy and carbon dioxide in space and time over the heterogeneous Barrax site, Int. J. Remote Sens., 29, 5215–5235, doi:10.1080/01431160802326099, 2008.

Timmermans, W. J., Bertoldi, G., Albertson, J. D., Olioso, A., Su, Z., and Gieske, A. S. M.: Accounting for atmospheric boundary layer variability on flux estimation from RS observations, Int. J. Remote Sens., 29, 5275–5290, doi:10.1080/01431160802036383, 2008.

van der Kwast, J., Timmermans, W., Gieske, A., Su, Z., Olioso, A., Jia, L., Elbers, J., Karssenberg, D., and de Jong, S.: Evaluation of the Surface Energy Balance System (SEBS) applied to ASTER imagery with flux-measurements at the SPARC 2004 site (Barrax, Spain), Hydrol. Earth Syst. Sci. Discuss., 6, 1165–1196, 2009, http://www.hydrol-earth-syst-sci-discuss.net/6/1165/2009/.

Wang, T.-I., Ochs, G. R., and Clifford, S. F.: A saturation-resistant optical scintillometer to measure Cn2, J. Opt. Soc. Am., 68, 334–338, 1978.

Watts, C. J., Chehbouni, A., Rodriguez, J.-C., Kerr, Y. H., Hartogensis, O., and de Bruin, H. A. R.: Comparison of sensible heat flux estimates using AVHRR with scintillometer measurements over semi-arid grassland in northwest Mexico, Agr. Forest Meteorol., 105, 81–89, 2000.

Wieringa, J.: Roughness-dependent geographical interpolation of surface wind speed averages, Q. J. R. Meteorol. Soc., 112, 867–889, 1986.

Wyngaard, J. C., Izumi, Y., and Collins, S. A.: Behavior of the refractive-index-structure parameter near the ground, J. Opt. Soc. Am., 61, 1646–1650, 1971.

Title Page
Abstract | Introduction
Conclusions | References
Tables | Figures
◀| |▶
◀ ▶
Back | Close
Full Screen / Esc
Printer-friendly Version
Interactive Discussion

Table 1. Correlation and Root Mean Squared Differences (RMSD) between aggregated LAS observations and reference values for sensible heat flux using different approaches.

Approach	Correlation (R^2)	RMSD $(\mathrm{W\,m^{-2}})$
0-D (V1)	0.28	81.6
0-D (WS)	0.12	113.7
1-D (V1-WS)	0.18	96.5
2-D (V1-WS-C2)	0.74	67.7

Title Page
Abstract
Introduction
Conclusions
References
Tables
Figures
◀◀
▶▶
◀
▶
Back
Close
Full Screen / Esc
Printer-friendly Version
Interactive Discussion

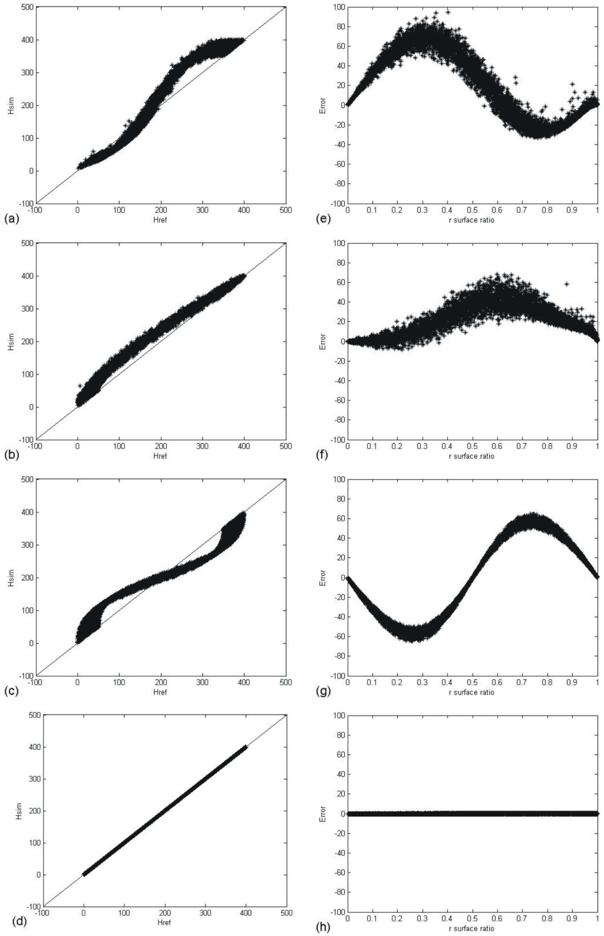

Fig. 1. Simulation results for a two-component surface using different approaches of aggregation.

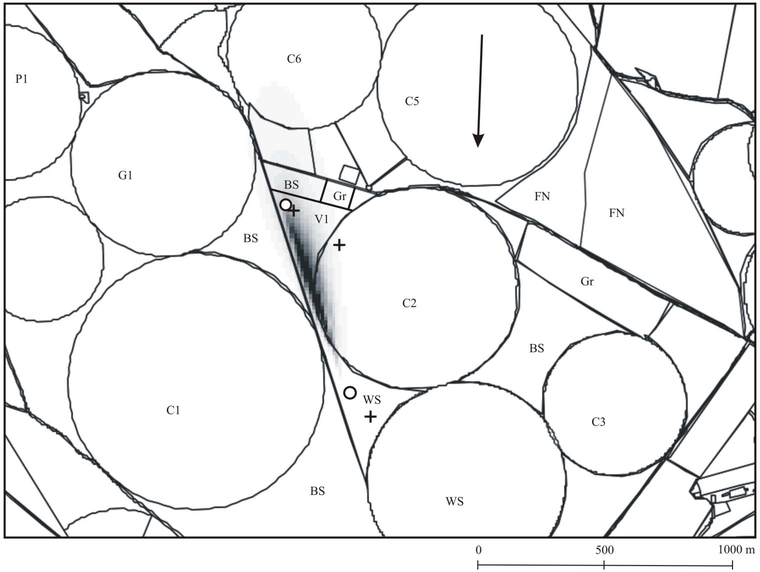

Fig. 2. Map (north oriented) of the experimental set-up at the Las Tiesas experimental farm, showing landcover units and scintillometer weighted observation source area. The LAS is represented by two white cirkels, and the sonic anemometers by (three) crosses, whereas an arrow indicates the wind direction. Letters represent landcovers vineyard ("V"), grass ("Gr"), corn ("C"), bare soil ("BS"), garlic ("G"), potato ("P") and forest nursery ("FN"), whereas the numbers refer to the respective field numbers.

Title Page
Abstract
Introduction
Conclusions
References
Tables
Figures
◀I
I▶
◀
▶
Back
Close
Full Screen / Esc
Printer-friendly Version
Interactive Discussion

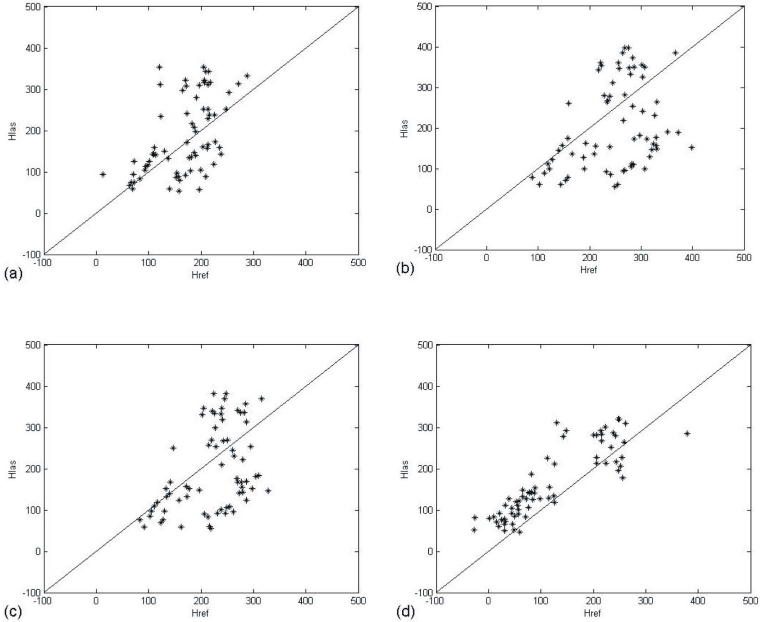

Fig. 3. Comparison between spatially-averaged sensible heat fluxes derived from sonic anemometers and scintillometry, using the 0-D (upper panels) and a 1-D and 2-D (lower left and lower right panel, respectively) approach for obtaining effective surface aerodynamic characteristics and reference flux values.

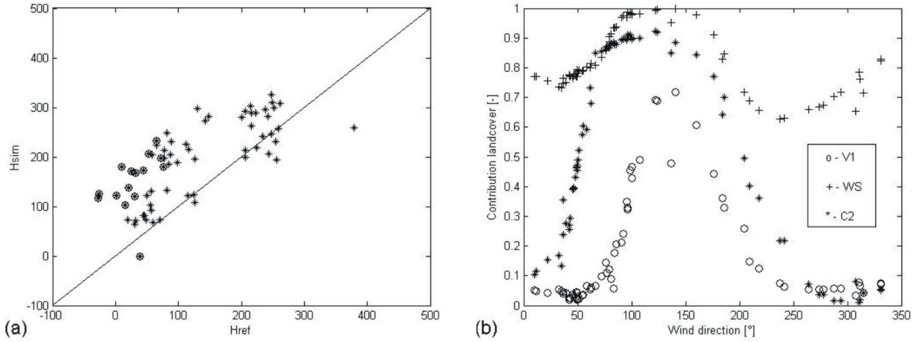

Fig. 4. Simulated versus reference fluxes, assuming known ratio of component fluxes. Influence of atmospheric stability contrast, stable by circles **(a)**, homogeneity of sonic footprints related to wind direction **(b)**.

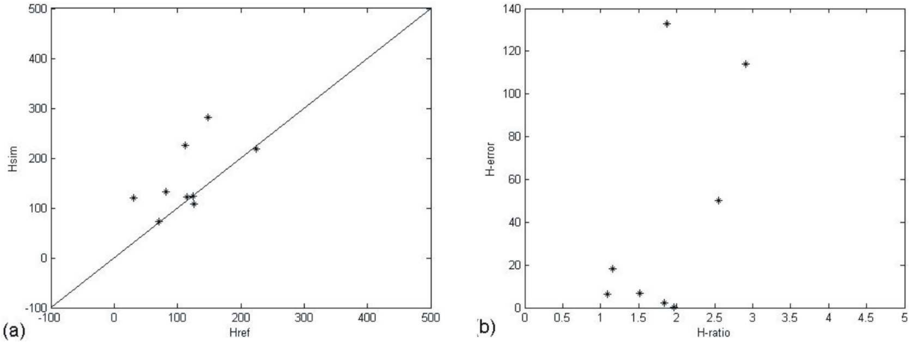

Fig. 5. Simulation results during south-eastern wind directions **(a)** and discrepancy between H_{las} and H_{ref} in relation to component flux contrast **(b)**.